Nuclear Instruments and Methods in Physics Research A 693 (2012) 268–275

Contents lists available at SciVerse ScienceDirect

Nuclear Instruments and Methods in Physics Research A

journal homepage: www.elsevier.com/locate/nima

Correction of optical aberrations in elliptic neutron guides

Phillip M. Bentley [a,b,*], Shane J. Kennedy [a], Ken H. Andersen [b], Damián Martin Rodríguez [c], David F.R. Mildner [d]

[a] Australian Nuclear Science and Technology Organisation (ANSTO), Locked Bag 2001, Kirrawee DC, NSW 2232, Australia
[b] European Spallation Source ESS AB, Box 176, 221 00 Lund, Sweden
[c] Jülich Centre for Neutron Science, Forschungszentrum Jülich GmbH, 52425 Jülich, Germany
[d] National Institute of Standards and Technology, Gaithersburg, MD 20899, USA

ARTICLE INFO

Article history:
Received 2 September 2011
Received in revised form
29 June 2012
Accepted 3 July 2012
Available online 13 July 2012

Keywords:
Neutron guide
Elliptic
Parabolic
Ballistic
Conic section

ABSTRACT

Modern, nonlinear ballistic neutron guides are an attractive concept in neutron beam delivery and instrumentation because they offer increased performance over straight or linearly tapered guides. However, like other ballistic geometries they have the potential to create significantly non-trivial instrumental resolution functions. We address the source of the most prominent optical aberration, namely coma, and we show that for extended sources the off-axis rays have a different focal length from on-axis rays, leading to multiple reflections in the guide system. We illustrate how the interplay between coma, sources of finite size, and mirrors with non-perfect reflectivity can therefore conspire to produce uneven distributions in the neutron beam divergence, a source of complicated resolution functions. To solve these problems, we propose a hybrid elliptic–parabolic guide geometry. Using this new kind of neutron guide shape, it is possible to condition the neutron beam and remove almost all of the aberrations, whilst providing the same performance in beam current as a standard elliptic neutron guide. We highlight the positive implications for neutron scattering instruments that this new shape can bring.

1. Introduction

Modern neutron guide systems increasingly feature a ballistic geometry, where the term "ballistic" refers to the middle section of the guide being wider than the guide entrance and exit. This widening reduces the number of reflections required to transport a neutron beam compared to a straight neutron guide of the same length, but it also introduces optical changes that add complexities that have only recently become apparent.

The first ballistic guides featured linearly tapered geometry for the converging and diverging sections [1,2]. Since this initial step, there has been progress [3] highlighting the benefits of switching to curved surfaces (or polygonal approximations to curves) following conic section geometries that have been exploited heavily in photon optics.

There are three types of conic section, depending on the properties of the beam and the desired result. For a perfectly implemented optical system, a *collimated* beam from an extended source can be focused onto a small target using a single reflection from a *parabolic* mirror.

On the other hand, *divergent* rays from a point source can be reflected by a single *elliptic* mirror from one focal point to another focal point with one reflection. This makes elliptic neutron guide shapes very attractive, as neutron beams are generally divergent at the source and we wish to minimise the number of reflections as far as possible to increase transport efficiency.

The third type of conic section is a *hyperbolic* shape that brings *convergent* rays to a nearer focal point. At grazing angles and large distances from the focal point, linearly tapered guides are good approximations to hyperbolic geometries because hyperbolic curves asymptotically approach straight lines.

For point sources or targets, consider the inversion of the optical system – i.e. interchanging the target for the source – it is clear that the properties of an ellipse are symmetric. For the other two mirror geometries, a parabolic mirror would reflect a divergent beam from a point source and produce parallel rays; and a hyperbolic mirror would reflect a divergent beam such that it appears to be radiating from a farther focal point.

While reflectivity is the essential issue for the development of neutron guides, optical problems can arise when trying to use conic sections in neutron optics. These can often be attributed to overlooking one or more of the following in the design:

1. Multiple reflections reduce the beam transport efficiency.
2. Neutron sources have finite spatial extent and cannot be treated as point sources.

* Corresponding author at: European Spallation Source ESS AB, Box 176, 221 00 Lund, Sweden.
Tel.: +46 46 888 30 87.
E-mail addresses: phillip.bentley@esss.se, phil.m.bentley@gmail.com (P.M. Bentley).

0168-9002/$ - see front matter © 2012 Elsevier B.V. All rights reserved.
http://dx.doi.org/10.1016/j.nima.2012.07.002

3. No single type of conic section mirror deals with all incoming trajectories effectively.
4. The optimal focal point of the geometry does not necessarily overlap with the intended source or target.

For example, it is very easy to design a ballistic guide system where the emerging beams have multi-modal divergence distributions at the sample position, which is the subject of this article. The root cause of this essentially includes all of the above, and this leads to a non-trivial resolution function, which could be problematic in some experiments.

In many cases, making simple changes to the operating conditions and geometry to take these principles into proper consideration can lead to a large improvement in the beam characteristics. This is an important issue, as elliptic guides are becoming very popular, almost to the extent that they are discussed in the context of being a "magic bullet" that is deployed to solve neutron transport problems where a different mirror geometry is probably more appropriate.

We illustrate how optical aberrations arise in elliptic neutron guides, and how to eliminate them. The beam modelling calculations have been performed using the established Monte-Carlo neutron ray tracing package VITESS [4] and a relatively new analytic method called "neutron acceptance diagram shading" (NADS) [5]. These are two different approaches. Aside from the statistical *vs.* analytic difference, NADS necessarily uses idealised, piecewise reflectivity curves with a sharp cut-off at the critical angle for reflection in the supermirrors (shown in Fig. 1). We define the magnitude of the neutron momentum transfer vector Q ($=4\pi\sin\theta/\lambda$), where θ is the angle of reflection and m is the critical momentum transfer for neutron reflection of the supermirror relative to that of natural nickel $Q_{Ni}=0.0217\ \text{Å}^{-1}$, so that the critical reflectivity of the supermirror is $Q_{crit}=mQ_{Ni}$. In the simplified model, the reflectivity decreases uniformly between Q_{Ni} and mQ_{Ni} according to

$$R(Q)=\begin{cases} R_{Ni}, & 0\le Q\le Q_{Ni} \\ R_{Ni}-g(Q-Q_{Ni}), & Q_{Ni}<Q\le mQ_{Ni} \\ 0, & Q>mQ_{Ni} \end{cases} \tag{1}$$

where

$$g=\frac{am^2}{(m-1)Q_{Ni}}. \tag{2}$$

This is simply an approximation to the performance of supermirror data from neutron guide manufacturers' web sites (e.g. http://www.swissneutronics.ch/products/coatings.html), for which $R_{Ni}\approx 0.98$ and modern coatings have $a\approx 0.01228$ giving $R_{crit}\approx 0.98-0.01228\ \text{m}^2$ as a good approximation for the reflectivity at the critical edge.

The Monte-Carlo method differs because it is possible to add more realistic details to the curve or even use a measured supermirror reflectivity profile. In this case, VITESS was used with more realistic, rounded reflectivity curves at Q_{Ni} instead of the piecewise function that Eq. (1) generates.

For a fair comparison, in this study we have restricted the maximum width in the middle of the guide to that of the parabolically tapered ballistic guide as studied by Schanzer et al. [3], i.e. 0.36 m, with the same total length of 50 m. We have modelled an 18.6 cm wide source similar to the Institut Laue-Langevin (ILL) horizontal cold source. The effects of coma are largely wavelength independent neglecting critical angles for reflection, but for illustration purposes we simulate three Maxwellian curves of characteristic temperatures of 163 K, 382 K and 37 K, and brightnesses 1.67×10^{13}, 3.97×10^{12} and 1.21×10^{13}, again matching the ILL horizontal cold source, and a relatively monochromatic beam at 4 Å. Our aim is to maximise the neutron beam current striking a sample of area $4\ \text{cm}\times 4\ \text{cm}$ without sacrificing the homogeneity of the phase space. As we are interested in relative changes, we ignore the vertical plane and concentrate on the effects of varying the geometry in the horizontal plane.

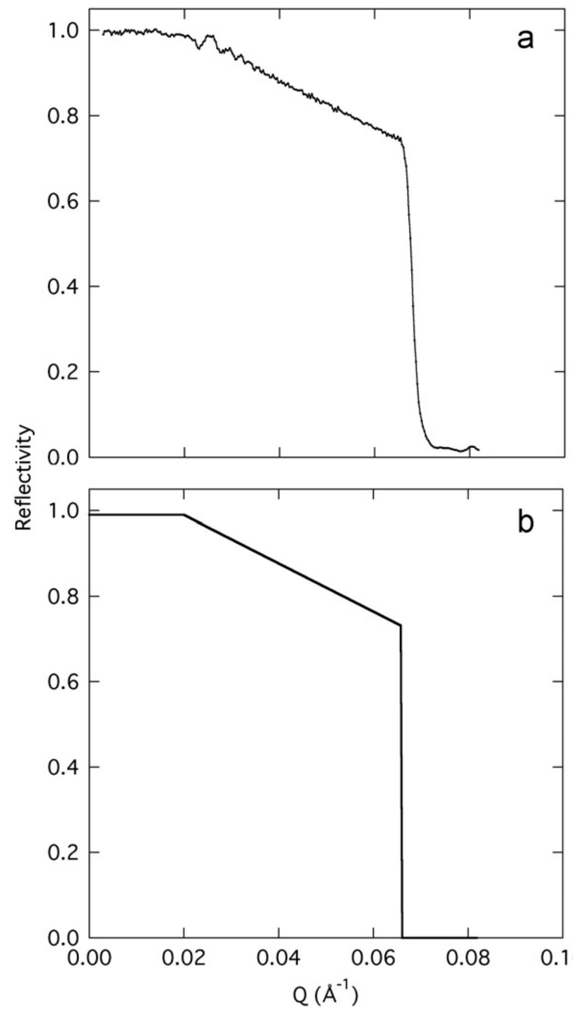

Fig. 1. (a) Measured reflectivity of an $m=3$ supermirror as a function of neutron momentum transfer, Q and (b) simplified model of the same supermirror using the same approximations that appear in NADS, after Bentley and Andersen [5]. Note that the critical reflectivity is rather poor for this particular mirror, which we use for illustration purposes, and that modern supermirrors offer much higher critical reflectivity.

This sample size is at the larger end of the range for neutron instruments, but beam homogeneity over such a breadth is an important design feature of spectrometers such as LET at ISIS [6], for example.

2. Elliptic guides

Schanzer et al. [3] compare a linearly tapered guide with a guide of the same geometry featuring parabolic tapering, and with a fully elliptical system. In the present study, we deal only with the parabolic version of the ballistic guide (henceforth referred to as "the ballistic guide") and the ellipse.

Fig. 2 shows a typical ballistic guide profile. This geometry produces an inhomogeneous, trimodal divergence distribution, shown in Fig. 3. When tracing backwards from the target, it becomes clear why there are two holes in the phase space.

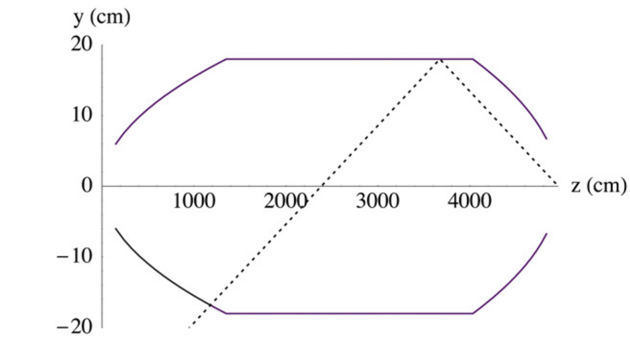

Fig. 2. Profile of the original ballistic guide for comparison with an ellipse, by Schanzer et al. [3]. The broken line is a reverse-traced trajectory corresponding to one of the two minima in the divergence profile at around 0.9° shown in Fig. 3.

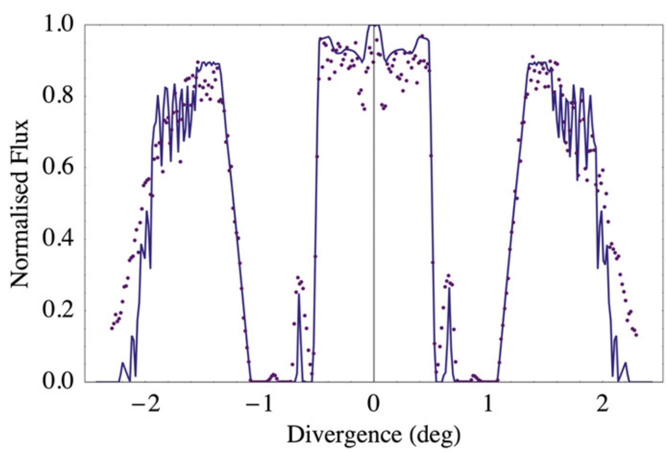

Fig. 3. The distribution of the beam divergence produced 0.5 m downstream of the exit of a ballistic guide similar to that shown in Fig. 2 integrated over a 4 cm wide sample. The solid lines are calculated using NADS [5] and the data points are computed using VITESS [4]. Both curves are normalised so that the beam at zero divergence (i.e. direct view of the source) has a relative flux of one. The sawtooth features in the data are caused by the use of short, straight sections of guide to approximate curved surfaces, and exaggerated by the idealised reflectivity curve.

The expanding parabola nearest to the source would have to reflect at large angles to supply this trajectory with a neutron.

Such a trimodal divergence profile has been observed before [7]. With three independent beams crossing at the sample, the angular component of the resolution function in one instrument plane might require at least six parameters—the angle of incidence and width of each beam component. Beyond the scope of this discussion, but worth bearing in mind, are the implications for chopper transmission functions in time-of-flight spectrometers because of the correlations between divergence and position in the guide phase space.

Note that simply increasing the m value does not completely solve the problem because at high-m and high angles the reflectivity is significantly lower than unity. Although the holes in phase space may be reduced in depth, they still remain. Ultimately, a more homogeneous beam requires a change in the geometry of the entire guide system.

The solution found by Schanzer is to exploit the geometry of an ellipse, shown in Fig. 4. As mentioned previously, an elliptic mirror has the property that any ray emitted from a point source at one focal point is reflected once and only once, and arrives precisely focused at the other focal point (neglecting gravity). Fig. 5 shows that the beam divergence distribution is much smoother in an elliptic guide compared to that of the ballistic guide in Fig. 3, even with a basic design featuring a

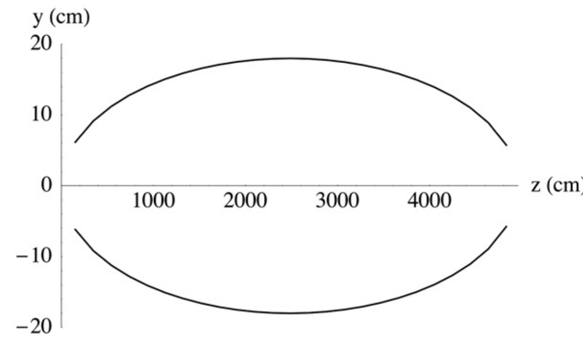

Fig. 4. Profile of an elliptic guide similar to that described by Schanzer et al. [3].

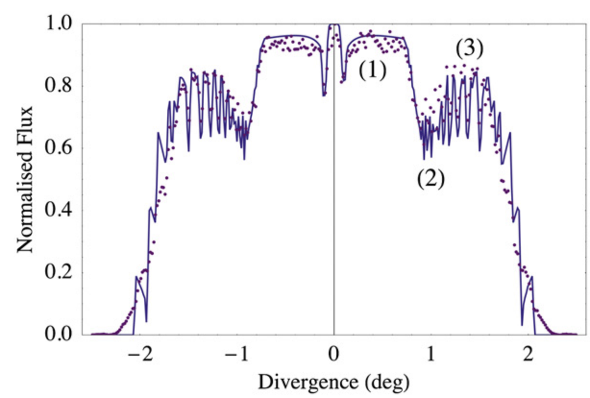

Fig. 5. The distribution of the beam divergence at the target position as produced by an elliptic guide integrated over a 4 cm wide sample. The solid lines are calculated using NADS and the data points are computed using VITESS. Both curves are normalised so that the beam at zero divergence (i.e. direct view of the source) has a relative flux of one. The sawtooth features in the data are caused by the use of short, straight sections of guide to approximate curved surfaces, and exaggerated by the idealised reflectivity curve. The groups of trajectories (1–3) are discussed later in the text.

uniform m value throughout the length of the guide. This smoothness or uniformity of the divergence distribution is what we refer to as "beam quality". In addition to the improvement in beam quality, the elliptic system provides a large increase in beam transport efficiency relative to the straight or ballistic system.

This improvement in beam quality can be expected *for some guide geometries*, but it would be a mistake to treat this result as a general case. We stress this point because firstly the parabolic–ballistic system in Schanzer's paper is not optimal. Secondly, linearly tapered guides can also be designed to reduce the problems shown in Fig. 3, and thirdly it is easy to misconfigure an ellipse such that it also produces very poor quality beams.

The elliptic divergence distribution shown here is a great improvement over the ballistic guide. Fig. 6 shows that it is still significantly worse than the beam quality produced by a straight guide. This is important because resolution calculations in neutron scattering often make idealised assumptions about the simple nature of the divergence distribution of the beam (see, for example, the article by Loong et al. [8]).

An examination of the full two-dimensional phase space using acceptance diagrams, in Fig. 7 reveals the significance of the minima at $\pm 1^\circ$. These are caused by gaps in the transmitted phase space, which occur when the first half of the ellipse cannot supply the second half of the ellipse with a neutron because the angles involved are greater than the maximum θ in the reflectivity curve. The gaps in this phase space could prove problematic

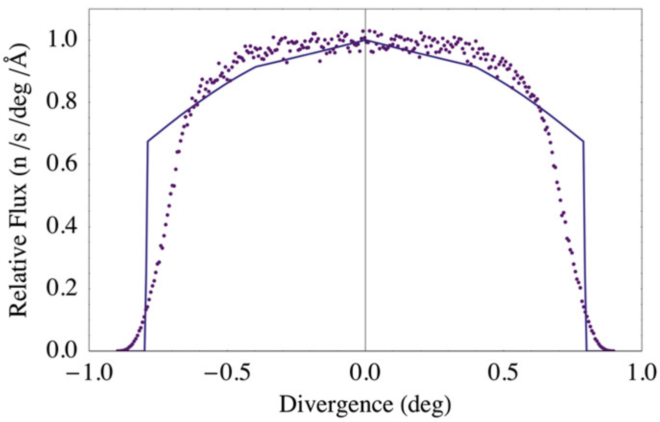

Fig. 6. Beam divergence distribution of a straight neutron guide integrated over a 4 cm wide sample. The solid lines are calculated using NADS and the data points are computed using VITESS. Both curves are normalised so that the beam at zero divergence (i.e. direct view of the source) has a relative flux of one.

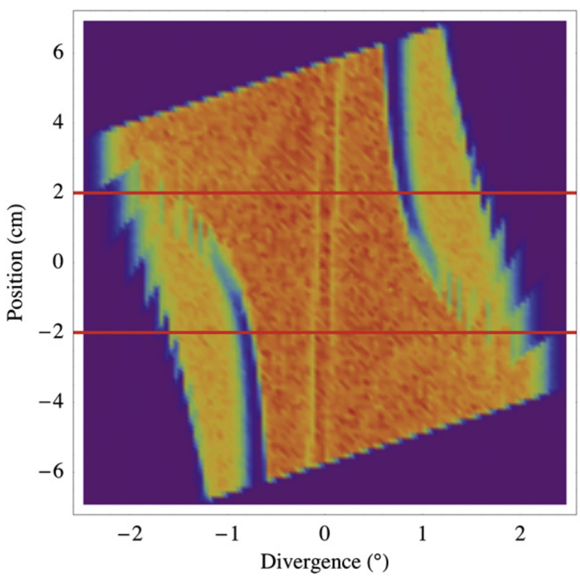

Fig. 7. Phase space at the sample plane 0.5 m downstream of the exit of the elliptic neutron guide computed using VITESS. The horizontal lines mark the spatial extent of a 4 cm wide sample.

for advanced instrument concepts that involve inclined or displaced mirrors with underlying elliptical shapes.

3. Coma in elliptic guides

One intrinsic problem with an elliptic neutron guide, and indeed any curved mirror, is the issue of coma. Coma is a well-understood phenomenon in reflecting optics. Early designs of reflecting telescopes, and cheap modern ones, produce images of star fields with sharp star images in the centre, but stars at the edges of the image are not well resolved. Instead, they appear to have tails resembling those of comets, hence the name "coma". Coma becomes a serious issue for neutron instrument resolution and background when one attempts a full design study of a neutron scattering instrument, such as small-angle neutron scattering instrument (SANS) [9].

Here, we do not derive coma strictly, but illustrate how the problem arises using Fig. 8. This compares two trajectories very simply, one from the leftmost focal point of an ellipse and the other from a point directly below at a distance $h/2$, to simulate the

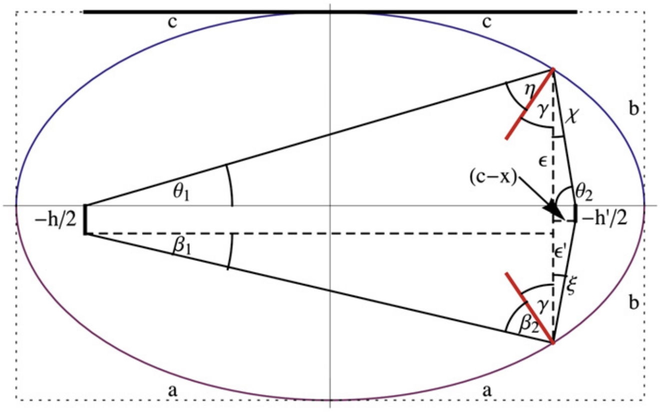

Fig. 8. The origin of coma in elliptic guides. The trajectory in the upper half plane of the figure shows a ray from an on-axis focal point source correctly focuses onto the opposite focal point. The lower half plane shows that a similar ray from an off-axis point on the source that is reflected at the same horizontal position x is not brought to the same focal point (where $x=0$ is at the ellipse centre). Rays reflected in the further half of the ellipse create a smaller blurred image of the source, whereas if rays were moving in the reverse direction reflecting in the near half of the ellipse they would create a large blurred image. The frame of the figure also shows the semimajor and semiminor axes a and b, and the half-distance between the foci, c.

effect of a source with height h. Navigating around Fig. 8 allows the derivation of the spatial extent of the image as a function of the location of the reflection in the horizontal direction x, which is valid in the small grazing angle regime for neutron guides

$$h' = 2\left\{\epsilon + (c-x)\tan\left[\tan^{-1}\left(\frac{h-2\epsilon}{2(c+x)}\right) + 2\tan^{-1}\left(\frac{c-x}{\epsilon}\right) + \tan^{-1}\left(\frac{\epsilon}{c-x}\right) + \tan^{-1}\left(\frac{\epsilon}{c+x}\right)\right]\right\} \tag{3}$$

where

$$\epsilon = \sqrt{b^2 - \frac{b^2x^2}{b^2+c^2}} \tag{4}$$

c is half the distance between the two foci (i.e. the distance from the ellipse center to a focus) given by $c^2 = a^2 - b^2$, and a and b are the semimajor and semiminor axes, respectively.

Eq. (3) is very well approximated [9] by

$$h' = h\cdot(c-x)/(c+x) \approx h\cdot(a-x)/(a+x) \tag{5}$$

because we are in the small angle regime and $a \approx c$ and $b \ll a,c$.

If an elliptic mirror were not to suffer from coma, then h'/h would be independent of x. Fig. 9 shows the x-dependence of h'/h, which can be interpreted as the spatial extent of the blurring caused by coma—a "coma size factor". The figure shows that the size of the coma-blurred image is greatest for rays close to the source, these neutrons experience multiple reflections. The image is smaller than the source for rays reflected near the target or sample. Only rays reflected in the very middle of the guide create a 1:1 scale image of the source.

With the source focus on the left and the sample focus on the right of Fig. 8, then Fig. 9 shows that for the rays striking the elliptic mirror close to the source, a 1 cm wide source would be expected to produce a blurred image with tails that are 20–50 cm wide.

The coma produces neutrons that strike the ellipse a second time further down the guide system, which indicates the problem with elliptic guides, namely the mismatch of the phase space between the first half of the ellipse and the second half of the ellipse, for rays that undergo multiple reflections increase the

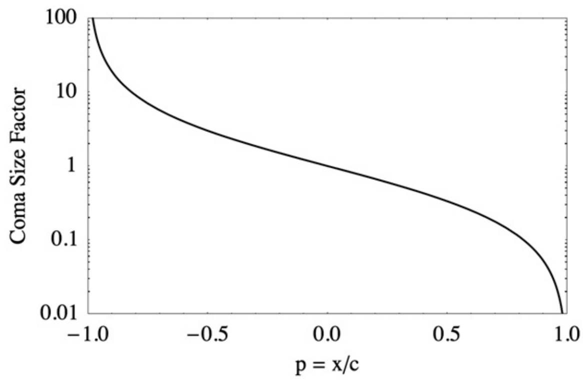

Fig. 9. Spatial extent of the coma blurring (h'/h) as a function of reflection position $p=x/c$. Here, we see that the worst coma effect is caused by rays striking the elliptic mirror close to the source, and after the mid-way point the coma effect is inverted so that the image is smaller than the source.

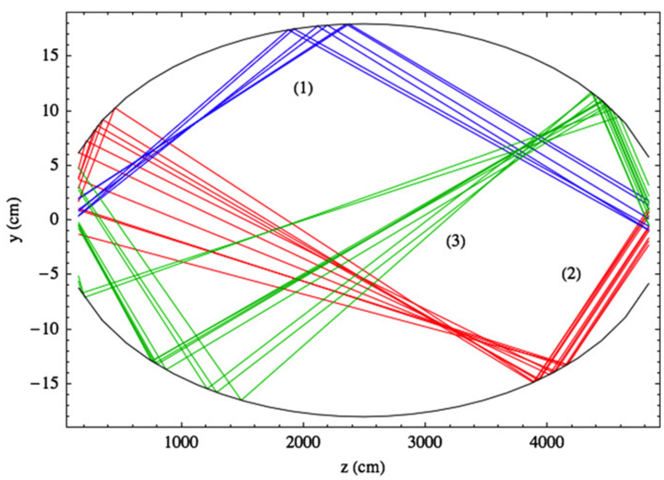

Fig. 10. Sets of neutron trajectories traced through an elliptic guide that match the final divergences labelled in Fig. 5.

coma significantly. This is what causes the vignetting features at high angles in Fig. 5, and we refer back to item 1 in the list of design problems in the Introduction section. Due to coma, the phase space is distorted in a way that an elliptical guide is not appropriate to transform it to the sample. This means that the later part of the guide should have another shape.

Referring back to Fig. 5, the central maximum is a direct view of the source, and the minima either side of this maximum, at just under 0.1°, are reflections at large grazing angles at the very entrance of the guide system. We have labelled three important features in this distribution that we can study in more detail by tracing the paths of neutrons with final divergences that match the locations of these features. This we have shown in Fig. 10. Coma is supplying trajectory set (2) with rays of neutrons that are reflected at very large grazing angles, causing the vignetting feature at $\pm 1^{\circ}$ in Fig. 5. The vignetting is of course amplified a little by our intentional use of only one m value throughout the system, but the data in Fig. 5 are not inconsistent with those in Schanzer's study. Trajectory set (1) exhibit the theoretical behavior of an elliptic guide, namely transport with one reflection. Trajectory set (3) are qualitatively similar to those of set (2), except that the performance is improved by having reflections at relatively small grazing angles nearer the middle of the guide system compared to those in set (2).

One possible solution to the coma problem is to make a pseudo-point source with an absorbing beam mask. This is not an ideal solution because the tails of the coma at the sample position still extend to many times the size of the mask aperture. More importantly, by masking the source, the incident flux is considerably reduced from its potential level by perhaps more than an order of magnitude, negating any flux benefits of using an elliptic guide over a straight guide.

For simplicity, we have ignored several other effects that contribute to the blurring of the image. Guide waviness is a minor perturbation that, for 50 m long guides, is expected to contribute a blurring of a few tens of millimeters or smaller – much smaller than the coma effect – but it does not change the underlying guide shape and therefore does not remove coma from the ellipse. It should be noted that varying m, or improving the polygonal approximation to the ellipse with many more straight sections, or even continuous mirrors, also do not change the underlying shape of the elliptic mirror and therefore do not remove the coma effect. We seek a more general solution to coma that can be applied to any elliptic guide deployment if required.

4. Eliminating elliptic guide aberrations

A far better solution would be to eliminate or reduce the effects caused by the aberration. In telescopes, this is achieved by carefully designing a secondary mirror to reduce or eliminate any optical aberrations caused by the primary mirror. Wolter [10] has designed a number of low grazing angle optical device types which serve precisely this purpose. They have been demonstrated to work excellently for both X-rays [11] and neutrons [12–14].

Our requirements in this study are not quite as strict. We are not necessarily interested in obtaining a point image of the beam, but improvements over elliptic guide systems to remove the multi-modality in the divergence distributions without compromising the beam transport performance of the system. To this end, we have experimented with several configurations of hybrid guide systems, where the first half of the guide has one particular conic section type, and the second part of the guide uses a different conic section type. A survey of the six possible permutations (elliptic–parabolic, elliptic–hyperbolic, parabolic–elliptic, parabolic–hyperbolic, hyperbolic–elliptic, and hyperbolic–parabolic) reveals that the elliptic–parabolic hybrid system offers the best performance for this particular case. This should not be treated as a general result—it is possible that a different combination of conic section offers better performance depending on the distances involved, and the spatial extent of the source and target. In any case, we will now focus our attention on this optimal elliptic–parabolic configuration (henceforth named "hybrid guide" for simplicity) and compare it with the current guide geometries. Fig. 11 illustrates this hybrid guide concept with an example that has the transition from ellipse to parabola at the mid point of the guide system.

To fully optimise a hybrid guide, there are more degrees of freedom than a regular elliptic guide:

1. The first focal point of the elliptic section.
2. The second focal point of the elliptic section.
3. The location of the transition from elliptic to parabolic shape.
4. The focal point of the parabola.
5. The maximum width of the guide.

The placement of the focal points do not necessarily have to coincide with the source and target, and in fact it is frequently optimal in neutron guides to have the focal points farther from the guide entrance/exit planes than the source and target.

The crossover point gives a degree of control on the homogeneity of the divergence profile from the guide system. In the limit of crossover at the guide exit, it is a purely elliptic system, and with the crossover at the guide entrance it is purely parabolic. Crossover in the exact middle of the guide, as shown in Fig. 11 provides a very high beam quality in terms of homogeneity in the divergence distribution. The full description of the hybrid guide parameters is given in Table 1. Fig. 12 is a schematic diagram showing these parameters on the optimised hybrid system.

The result of these slight changes is apparent in Fig. 13, which shows that our hybrid system has a much smoother divergence distribution. Indeed, the beam quality is comparable to that of a straight neutron guide, shown in Fig. 6, although it matches the elliptic guide for both divergence and high beam transport.

The overall phase space for the hybrid guide in Fig. 14 is more homogeneous compared to that of the elliptic guide in Fig. 7, even for off-axis positions and at high angles of divergence.

In Fig. 15 we have repeated for the hybrid geometry system similar ray calculations shown in Fig. 10 for the elliptic guide. Here, we see that where trajectory set (2) suffered from zigzag reflections in the ellipse with a large grazing angle, now with a parabolic mirror near the sample this part of the phase space is imaging the source with only one reflection. Trajectories (1) and (3) remain similar to those in the pure ellipse case.

Fig. 16 compares the on-sample flux performance of each of the guide geometries that have been modelled, assuming the 4 cm wide sample 0.5 m downstream from the guide exit. Here, we see that the ellipse and the hybrid have similar flux gains relative to the simple, straight guide, and the hybrid geometry may even have a slight edge over the ellipse. The gains of course come from an increased divergence of the beam, so a fair comparison must also take into consideration the useful

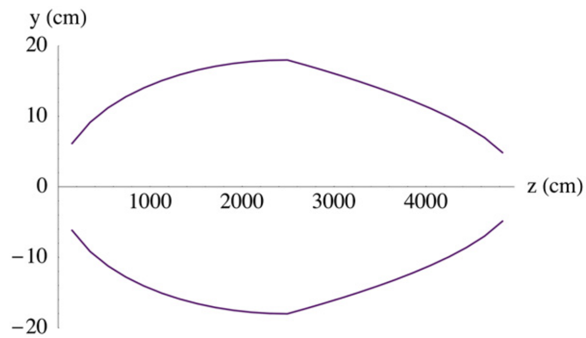

Fig. 11. Profile of a hybrid guide, with the crossover from ellipse to parabola in the midpoint of the system.

Table 1
Parameters found for the optimised hybrid guide. Focal points are labelled in parenthesis with the same symbols as those used in Fig. 12.

Parameter	Value (m)
Elliptic focal point 1 (F_1)	−3.5
Source position	−1.5
Entrance to elliptic guide	0
Elliptic focal point 2 (F_2)	48.1
Crossover point	23.4
Parabolic guide exit	46.8
Target	47.3
Parabolic focal point (P)	48.1
Maximum width at widest point	0.36

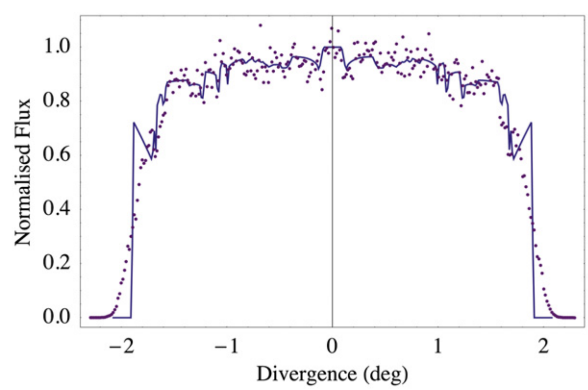

Fig. 13. Beam divergence distribution at the target position as produced by the hybrid guide. The solid lines are calculated using NADS and the data points are computed using VITESS. Both curves are normalised so that the beam at zero divergence (i.e. direct view of the source) has a relative flux of one. The sawtooth features in the data are caused by the use of short, straight sections of guide to approximate curved surfaces, and exaggerated by the idealised reflectivity curve.

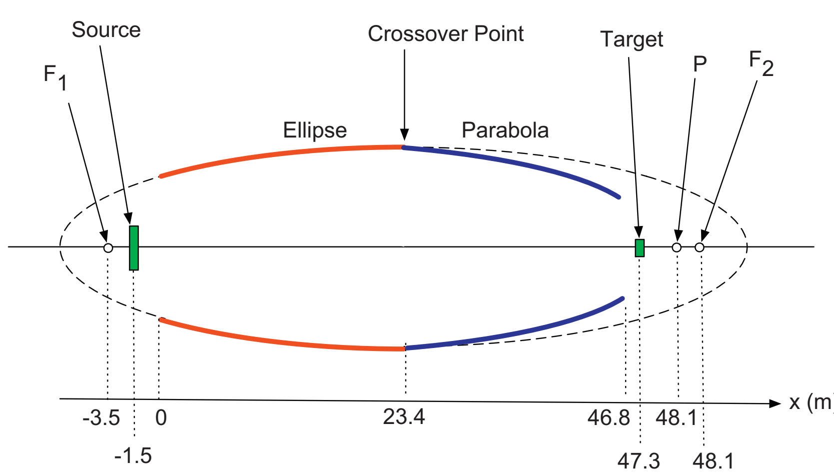

Fig. 12. Schematic of a hybrid guide illustrating the values of the parameters in Table 1. Distances along the length of the guide are given in metres. The elliptic part is on the left (red in colour); the parabolic part is on the right (blue in colour); and the dotted line is a full ellipse that overlaps with the geometry of the elliptic section. Note that we are illustrating the parabolic focal point P and the second elliptic focal point F_2 as separate, independent points in this figure, but in our simulations they are at the same distance of 48.1 m from the entrance of the elliptic guide. (For interpretation of the references to color in this figure caption, the reader is referred to the web version of this article.)

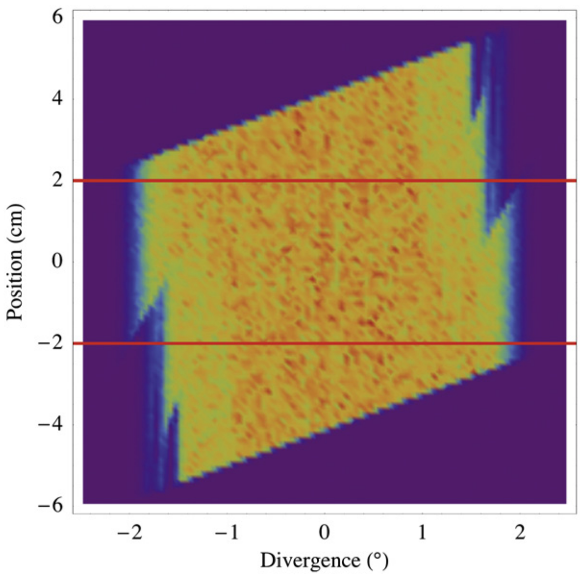

Fig. 14. Phase space at the sample plane 0.5 m downstream of the exit of the hybrid neutron guide computed using VITESS. The horizontal lines mark the spatial extent of a 4 cm wide sample.

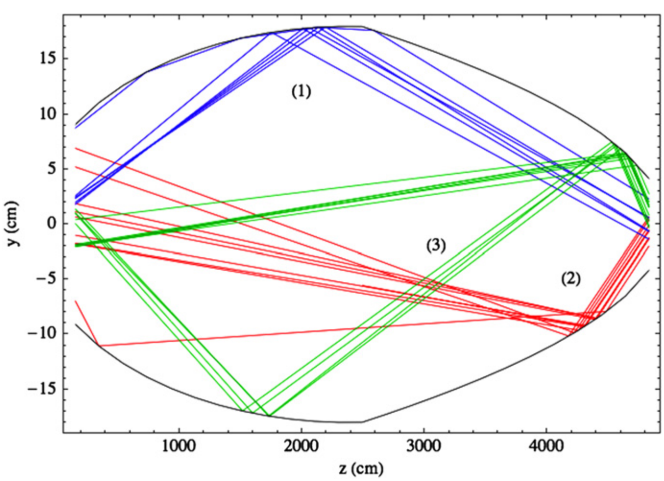

Fig. 15. Sets of neutron trajectories traced through a hybrid guide, with the same divergences as those in Fig. 10 matching features in Fig. 5. The majority of the trajectories in set (2) now image the source with one reflection from the parabolic mirror, rather than two reflections with a large grazing angles as they do in the elliptic system.

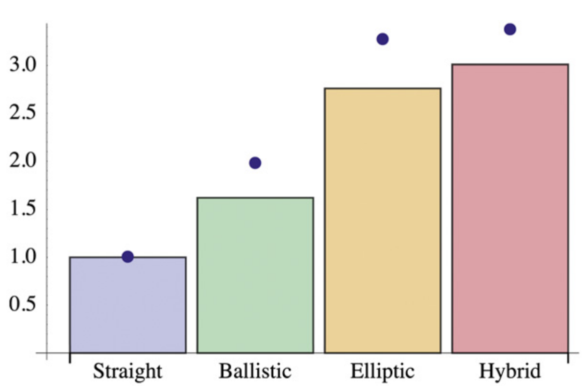

Fig. 16. On-sample calculated flux for each of the geometries relative to the straight guide, for the same length. The bars are the performance as calculated using NADS, the points were calculated using VITESS.

divergence of a spectrometer coupled to the guide, bearing in mind the divergence distributions in Figs. 5, 6 and 13.

Despite the fact that a hybrid guide was designed around the acceptance of multiple reflections in elliptic guide systems, we see that the parabolic section can be effective in removing the elliptic guide vignetting by reducing the number of reflections in the system compared with a purely elliptic guide. At the same time, the parabolic mirror deals effectively with multiple reflections. This is not surprising when one considers the understanding of aberrations that is employed in Wolter optics and modern reflecting telescope design. What is surprising here, in the context of neutron guides, is that the best performance is achieved by using principally the *worst* part of the ellipse for optical aberrations. With a little further examination, however, this hybrid system becomes very logical.

In the purely elliptic case, the coma is not corrected by these subsequent reflections; an ellipse is most efficient at reflecting trajectories from the point source, but not from the off-axis regions. In contrast, a hybrid system presents these relatively collimated rays with a parabolic section, which focuses the rays very effectively onto the sample. It should be noted that inverting the system by arranging the parabolic mirror to be near the sample, followed by an elliptic section, does not perform as well as the elliptic–parabolic hybrid described here.

5. Conclusions

We have shown that the vignetting in elliptic neutron guides, brought about by coma, can be greatly reduced by using a hybrid geometry where the second section of the guide is parabolic. Such hybrid elliptic–parabolic guides are expected to be of interest in a wide range of applications, either as a primary beam delivery system or as a means of focusing a moderately diverging beam onto a sample or virtual source.

We are particularly interested in the effect upon time-of-flight and diffraction applications, for which the beam homogeneity provides a relatively simple angular resolution function, and also a simple convolution with chopper openings. Both of these scenarios are likely to be served better by a hybrid system than a pure elliptic system.

An example where hybrid guides should excel is in backscattering spectrometers of the IN16 type [15], where the beam divergence distribution function maps onto the instrument dynamic range, and any inhomogeneities in the beam divergence (such as the minima in Figs. 3 and 5) directly affect the quality of the instrument's data.

Acknowledgements

The authors are indebted to all the participants of the ANSTO-NIST instrumentation design workshop that ran for the month of November 2009 at NIST, Gaithersburg MD, USA. In particular, we thank our host Rob Dimeo, NIST scientists Jeremy Cook, John Copley, and John Barker; and the delegates from ANSTO: Anna Sokolova, Nicolas de Souza, Frank Klose and Oliver Kirstein. We would also like to thank Rohland Gähler (Institut Laue Langevin), and Gary McIntyre (ANSTO) for useful discussions. Mention of specific commercial products is for informational purposes only and does not constitute endorsement by the National Institute of Standards and Technology. This work was presented at International Workshop on Neutron Optics "NOP2010" in Alpe d'Huez, France, and the delegates are thanked for their constructive feedback at this event.

References

[1] F. Mezei, Journal of Neutron Research 6 (1997) 3.
[2] H. Abele, D. Dubbers, H. Häse, M. Klein, A. Knöpfler, M. Kreuz, T. Lauer, B. Märkisch, D. Mund, V. Nesvizhevsky, A. Petoukhov, C. Schmidt, M. Schumann, T. Soldner, Nuclear Instruments and Methods in Physics Research Section A (2006) 407.
[3] C. Schanzer, P. Böni, U. Filges, T. Hils, Nuclear Instruments and Methods in Physics Research Section A 529 (2004) 63.
[4] D. Wechsler, G. Zsigmond, F. Streffer, F. Mezei, Neutron News 11 (4) (2000) 25. 〈http://www.hmi.de/projects/ess/vitess/〉.
[5] P.M. Bentley, K.H. Andersen, Nuclear Instruments and Methods in Physics Research Section A 602 (2008) 564.
[6] R.I. Bewley, J.W. Taylor, S.M. Bennington, Nuclear Instruments and Methods in Physics Research Section A 637 (2011) 128.
[7] I.N. Goncharenko, I. Mirebeau, P. Molina, P. Böni, Physica B 234–236 (1997) 1047.
[8] C.-K. Loong, S. Ikeda, J.M. Carpenter, Nuclear Instruments and Methods in Physics Research Section A 260 (1987) 381.
[9] D.M. Rodriguez, S.J. Kennedy, P.M. Bentley, Journal of Applied Crystallography 44 (2011) 727.
[10] H. Wolter, Annalen der Physik 445 (1952) 94.
[11] M.C. Weisskopf, B. Brinkman, C. Canizares, G. Garmire, S. Murray, L.P. van Speybroeck, Publications of the Astronomical Society of the Pacific 114 (2002) 1.
[12] M.V. Gubarev, B.D. Ramsey, D.E. Engelhaupt, J.M. Burgess, D.F.R. Mildner, Nuclear Instruments and Methods in Physics Research Section B 265 (2007) 626.
[13] D.F.R. Mildner, M.V. Gubarev, Nuclear Instruments and Methods in Physics Research Section A 634 (2011) S7.
[14] B. Khaykovich, M.V. Gubarev, Y. Bagdasarova, B.D. Ramsey, D.E. Moncton, Nuclear Instruments and Methods in Physics Research Section A 631 (2011) 98.
[15] B. Frick, A. Magerl, Y. Blanc, R. Rebesco, Physica B 234–236 (1997) 1177.